# THE STEFAN PROBLEM WITH NONLINEAR KINETIC UNDERCOOLING

*by* J. D. EVANS

(*Department of Mathematical Sciences, University of Bath, Bath* BA2 7AY)

*and* J. R. KING

(*Department of Theoretical Mechanics, University of Nottingham, Nottingham* NG7 2RD)

[Received 21 September 2001. Revise 27 June 2002]

**Summary**

The behaviour of the one-phase Stefan problem with nonlinear kinetic undercooling is studied. This system is physically relevant in a number of contexts, in particular as the sharp-interface (fast-reaction) limit of a variety of reaction–diffusion systems. The similarities and differences with the linear kinetic condition (studied by Evans and King (2000)) are highlighted for both one- and two-dimensional problems. Asymptotic results (both in time and in the Stefan number) are obtained for the power-law form of the kinetic condition. Significantly, the one-dimensional growth behaviour of the moving boundary is seen to be relatively insensitive to the precise form of the nonlinear kinetic condition, and this in effect has hindered its experimental determination in applications such as silicon oxidation. By contrast, the two-dimensional development of the moving boundary around a mask edge depends strongly on the form of the kinetic condition and consequently a method, similar to the Boltzmann–Matano method for determining nonlinear diffusivities, is described to determine the kinetic undercooling relation from experiment.

## 1. Introduction

In Evans and King (**1**), the one-phase Stefan problem with kinetic undercooling was studied with a linear kinetic condition at the moving boundary. A number of transformations and asymptotic results (for small and large time and Stefan number) were presented in one dimension and for a mask edge problem in two dimensions. Here we extend these results by considering a more general nonlinear kinetic condition on the moving interface. The kinetic condition relates interface undercooling to interface growth rate and nonlinear relationships are seen in the modelling of certain heat and mass transfer problems involving non-equilibrium phase change. In crystal growth, Kirkpatrick *et al.* (**2**) and Worster and Kerr (**3**) indicate that algebraic and exponential forms for the dependence of the undercooling on the interface growth rate are commonly found from fits with experimental data. Similar forms are reported in Crowley (**4**) for the additional applications of pulsed annealing, cellular alloy solidification and solid fuel combustion. Importantly, as noted in (**1**), the Stefan problem with kinetic undercooling is relevant to the penetration of solvents in glassy polymers (**5** to **9**) and the oxidation of silicon (**10**, **11**)). In the polymer application, a power-law kinetic condition is usually imposed at the moving interface, whilst in silicon oxidation, although a linear condition is most commonly adopted, similar nonlinear power-law forms have been suggested by Blanc (**12**) and Hu (**13**) and equivalent formulations are pertinent to the description of many

© Oxford University Press 2003; all rights reserved.


Downloaded from https://academic.oup.com/qjmam/article/56/1/139/1836811 by guest on 21 August 2022

other reacting systems. Although nonlinear bulk reaction kinetics are widely studied (in the form of reaction–diffusion systems), nonlinear surface reaction models (which are formulated as sharp-interface (moving-boundary) problems) are thus equally important and relevant (cf. (**14**)).

The above mentioned applications provide the motivation for the study of nonlinear kinetic undercooling. A discussion of the underlying physics can be found in (**2**) for crystal growth, the references cited in (**4**, pp. 650–656) for cellular alloy solidification and solid fuel combustion, (**13**, **15**) for silicon oxidation and (**5**) for polymer-solvent systems. In these applications, the kinetic condition is typically regarded as a phenomenological relation and its precise form is often claimed to be crucial in distinguishing distinct behaviours of the interface evolution (cf. (**5**)). When definiteness is required, power-law and exponential relations are usually adopted (see equations (6) and (7) below). Reference (**14**) provides a discussion of the relationship between bulk and surface reaction kinetics in the fast-reaction limit, illustrating the relevance to a wide range of reacting systems of the formulation studied below.

Although not pursued here, it is worth mentioning that in two or three space dimensions, surface tension effects also become important. These are usually incorporated through a Gibbs–Thomson relation, where the equilibrium temperature or concentration of the phase-change interface is related to its mean curvature; see, for example, Schaeffer and Glicksman (**16**) or Umantsev and Davis (**17**) for heat transfer problems and Mullins and Serkerka (**18**) or Langer (**19**) for mass transfer. Generally, a linear dependence on the interface curvature is used, for example, (**20** to **26**). However, Abergel *et al.* (**27**) and Scheid (**28**) consider a nonlinear (exponential) dependence, which follows from the use of Nernst's law for the kinetics of dissolution and growth of a solid phase in a solid–liquid system.

The structure of the paper is as follows. In section 2 we address the one-dimensional problem, recording the similarities and differences from the linear case considered in (**1**). A note is made of the transformations that carry over and the generalizations of the asymptotic approximations for small and large time as well as small and large Stefan number. In the case of a power-law kinetic condition, the limiting asymptotic solution behaviour is derived for the two extreme limits of the power-law exponent. Section 2 ends with an illustration of the numerical solution and a discussion on the qualitative comparison with some of the asymptotic approximations derived. In section 3, two-dimensional behaviour is examined through consideration of a mask edge problem. As in (**1**), the reaction-controlled limit is considered and its large-time behaviour analysed for the power-law kinetic condition, illustrating the generalization from the linear case and the contrasting results that can be obtained as the power-law exponent is varied. In the Appendix, remarks are made considering nonlinear diffusion with a more general regularization, incorporating surface tension, introduced on the moving boundary.

## 2. The one-dimensional problem

### 2.1 *Formulation*

We consider here the one-phase Stefan problem with nonlinear kinetic undercooling at the free boundary. The one-phase problem is a relevant approximation to the two-phase problem, when, for one of the phases the conductivity (in the case of heat transfer) or the diffusion coefficient (in mass transfer problems) is small relative to that of the other phase; in contexts such as silicon oxidation, however, it should be stressed that there is no corresponding two-phase problem since the oxidant reacts rapidly with the silicon whenever it encounters it. Following (**1**), in the one-dimensional case

Downloaded from https://academic.oup.com/qjmam/article/56/1/139/1836811 by guest on 21 August 2022

the problem may be stated in dimensionless form as:

$$\text{in } 0 < x < s(t) \qquad \frac{\partial u}{\partial t} = \frac{\partial^2 u}{\partial x^2}, \tag{1}$$

$$\text{on } x = s(t) \qquad \lambda \dot{s}(t) = F(u), \quad \frac{\partial u}{\partial x} = -(u + \lambda)\dot{s}(t), \tag{2}$$

$$\text{on } x = 0 \qquad u = 1, \tag{3}$$

$$\text{at } t = 0 \qquad s = 0, \tag{4}$$

where (adopting terminology appropriate to problems of heat transfer) $u(x, t)$ denotes the temperature in the liquid, which occupies the region $0 \leqslant x \leqslant s(t)$, $s(t)$ denotes the position of the unknown moving boundary and $\lambda = L/cU$ is the Stefan number, where $L$ is the latent heat, $c$ is the specific heat capacity of the liquid and $U$ is a representative temperature scale. A Dirichlet condition is posed on the fixed boundary $x = 0$. The interpretation of this system in the context of silicon oxidation and polymer-solvent systems is given in (**1**). Because we fix $s(0) = 0$, there is no externally-imposed length scale and the scaling we adopt fixes the dimensionless kinetic undercooling parameter to be $\lambda$; if $s(0)$ is sufficiently large, however, kinetic undercooling effects are negligible (cf. the discussion below of the large-time behaviour), but this is not the case for many of the applications of concern here (notably silicon oxidation, where sub-micron lengthscales pertain).

The nonlinear kinetic undercooling term is represented by the function $F$, which is assumed to have the following properties:

$$F(u) \in C^1(0, 1], \qquad F'(u) > 0 \text{ for } u \in (0, 1], \qquad F(0) = 0. \tag{5}$$

Only problems in which the moving boundary is advancing will be treated, the form of the second condition in (2) requiring (as described in (**1**)) $\dot{s} \geqslant 0$; the case $\dot{s} < 0$, when a different condition holds in the one-phase limit that we are concerned with here, will be addressed elsewhere. The commonly proposed forms are a power-law relation

$$F(u) = u^{1/n}, \quad n > 0, \tag{6}$$

and exponential

$$F(u) = e^{ku} - 1, \quad k > 0, \tag{7}$$

with $k$ a dimensionless constant. The power-law form with $n = \frac{1}{2}$ has been proposed for certain melts in crystal growth (**2**, **3**) and cellular alloy solidification (**4**). In silicon oxidation (**12**) suggests $n = 2$ whilst (**13**, **15**) suggest a more general power in the range $1 \leqslant n \leqslant 2$. In polymer-solvent systems, Astarita and Joshi (**5**) suggest the range $\frac{1}{3} \leqslant n < \frac{1}{2}$. The exponential form is applicable to solid fuel combustion (**4**) and may also be to some specific types of crystal growth (**2**). The wide range of values for the power $n$ indicates that the limits of both $n$ small and $n$ large are worth investigating to obtain a clear picture of the range of behaviour which can be exhibited.

The first condition in (2) can be rewritten as

$$u = G(\lambda \dot{s}(t)), \tag{8}$$

Downloaded from https://academic.oup.com/qjmam/article/56/1/139/1836811 by guest on 21 August 2022

where $G = F^{-1}$ also satisfies the properties in (5). For use in later sections, we define

$$a \equiv F(1)\,, \qquad b \equiv F'(1) \tag{9}$$

and where numerical computations are involved, the power-law form (6) will be chosen. Fasano *et al.* (**29**) establish well-posedness and regularity of the moving boundary for (1) to (4) with $F$ satisfying (5). Corresponding results have been obtained by Andreucci and Ricci (**30**) when a Neumann condition replaces the Dirichlet condition (3). The numerical scheme described in (**29**) will be used to illustrate the asymptotic results of later sections. In the case of a linear kinetic term, Gröger and Strecker (**31**) have shown existence and uniqueness for this problem in the context of silicon oxidation.

In the corresponding two-phase non-equilibrium problems in one dimension, existence and uniqueness results have been obtained in (**32** to **35**) for a linear kinetic undercooling term. In the nonlinear case, Visintin (**36**) and Guan and Wang (**37**, **38**) have demonstrated existence, with the latter authors placing constraints on the growth of the function $F(u)$. In (**33**) results were obtained for higher dimensions with surface tension also included.

### 2.2 *Transformations and conservation laws*

The transformation

$$v(x,t) = -\int_x^{s(t)} (u(x',t) + \lambda)\, dx', \tag{10}$$

noted by Fasano *et al.* (**29**), is applicable to the nonlinear kinetic undercooling case and gives what can be viewed as a generalized one-phase ablation problem, namely

$$\text{in } 0 < x < s(t) \qquad \frac{\partial v}{\partial t} = \frac{\partial^2 v}{\partial x^2}, \tag{11}$$

$$\text{on } x = s(t) \qquad v = 0, \qquad \frac{\partial v}{\partial x} = \lambda + G(\lambda \dot{s}(t)), \tag{12}$$

$$\text{on } x = 0 \qquad \frac{\partial v}{\partial x} = 1 + \lambda, \tag{13}$$

$$\text{at } t = 0 \qquad s = 0. \tag{14}$$

By contrast, the Duvaut transformation, valuable for linear kinetics (see (**1**)), is of very limited use in the current context. The conservation relation

$$\int_0^{s(t)} (u(x,t) + \lambda)\, dx + \int_0^t \frac{\partial u}{\partial x}(0,t')\, dt' = 0 \tag{15}$$

of course remains valid in the nonlinear case, but the result for the first moment becomes

$$\int_0^{s(t)} x\,(u(x,t) + \lambda)\, dx + \int_0^t G(\lambda \dot{s}(t'))\, dt' - t = 0, \tag{16}$$

which is of limited value other than for linear kinetics.

Downloaded from https://academic.oup.com/qjmam/article/56/1/139/1836811 by guest on 21 August 2022

2.3 *Asymptotic behaviour for small and large times*

For small time, the asymptotic results

$$s(t) = a\,\frac{t}{\lambda} - \frac{a^2 b}{2}\left(1+\frac{1}{\lambda}\right)\frac{t^2}{\lambda^2} + O(t^3), \tag{17}$$

$$u(x,t) = 1 - \left(1+\frac{1}{\lambda}\right) a\,x + O(t^2) \qquad \text{for } x = O(t),\ 0 < x/t < a/\lambda, \tag{18}$$

are readily deduced, where $a$ and $b$ are defined in (9). The large-time behaviour is given by

$$s(t) \sim 2\alpha\sqrt{t} + s_1(t), \tag{19}$$

$$u(x,t) \sim 1 - \frac{\operatorname{erf}\left(x/2\sqrt{t}\right)}{\operatorname{erf}(\alpha)} + u_1(x,t) \qquad \text{as } t \to \infty, \tag{20}$$

where $s_1(t) = o(\sqrt{t})$ and $u_1 = o(1)$ as $t \to \infty$ are the correction terms. At leading order the kinetic term is negligible, so that the dominant behaviour in (19), (20) is given by the Neumann solution to the classical Stefan problem, with $\alpha$ given by the only positive root of the transcendental equation

$$\sqrt{\pi}\alpha e^{\alpha^2}\operatorname{erf}(\alpha) = 1/\lambda. \tag{21}$$

If

$$F(u) \sim u^{1/n} \qquad \text{as } u \to 0 \tag{22}$$

then the first correction terms can be calculated explicitly when $n < 2$ giving

$$s_1(t) \sim -\beta t^{(1-n)/2}, \tag{23}$$

$$u_1(x,t) \sim t^{-n/2} f_n(\eta) \qquad \text{as } t \to \infty, \tag{24}$$

with

$$\eta = \frac{x}{2\sqrt{t}}, \qquad f_n(\eta) = \left((\lambda\alpha)^n - \lambda\alpha\beta\right) e^{(\alpha^2-\eta^2)/2}\left(\frac{U(\sqrt{2}\eta)V(0) - V(\sqrt{2}\eta)U(0)}{U(\sqrt{2}\alpha)V(0) - V(\sqrt{2}\alpha)U(0)}\right),$$

$$\beta = \lambda^{n-1}\alpha^n\left(\frac{\alpha\left(U(\sqrt{2}\alpha)V(0) - V(\sqrt{2}\alpha)U(0)\right) + \sqrt{2}\left(U'(\sqrt{2}\alpha)V(0) - V'(\sqrt{2}\alpha)U(0)\right)}{\alpha\left(U'(\sqrt{2}\alpha)V(0) - V'(\sqrt{2}\alpha)U(0)\right) + \lambda(\alpha^2+1-n)\left(U(\sqrt{2}\alpha)V(0) - V(\sqrt{2}\alpha)U(0)\right)}\right),$$

where

$$U(\xi) = D_{n-1}(\xi), \qquad V(\xi) = \frac{\Gamma(1-n)}{\pi}\left(\cos(\pi n)D_{n-1}(\xi) + D_{n-1}(-\xi)\right),$$

with $D_{n-1}(\xi)$ being a parabolic cylinder function. These terms are independent of the earlier evolution and we note the simplification which occurs when $n = 1$, whereby $s_1 = -1$ and

Downloaded from https://academic.oup.com/qjmam/article/56/1/139/1836811 by guest on 21 August 2022

$u_1 = O(t^{-1})$ rather than $O(t^{-\frac{1}{2}})$ due to $\beta = 1$ holding in this case, so that $f_1(\eta) \equiv 0$; which is not a coincidence, the result following most directly from the Baiocchi transformed version of the problem (which is available only in the case $n = 1$). When $n > 2$ we have $s_1 = O(t^{-\frac{1}{2}})$ and $u_1 = O(t^{-1})$, it only being possible to determine the coefficients of these terms numerically; they depend on the initial data if (4) is generalized and correspond to translations of $t$ in the leading-order solution (so still correspond to the classical Stefan problem).

### 2.4 *The limits of small and large Stefan number*

2.4.1 *Large Stefan number.* In the limit of large Stefan number ($\lambda \to \infty$), we rescale $t = \lambda\tau$ and expand in inverse powers of $\lambda$. The leading-order problem is quasi-steady and, writing

$$s(\tau) = s_0(\tau) + O\left(1/\lambda\right), \qquad u(x,\tau) = u_0(x) + O(1/\lambda), \tag{25}$$

the solution can be written parametrically in terms of $p(\tau)$, given by

$$\tau = \frac{1}{2}\left(\frac{1}{p^2} + \frac{1}{a^2}\right) - \frac{G(p)}{p^2} + \int_p^a \frac{G(p)}{p^3}\,dp \tag{26}$$

(with, since $G(a) = 1$, $p = a$ at $\tau = 0$), in the form

$$u_0 = 1 - px\ , \qquad s_0 = \frac{1}{p} - \frac{G(p)}{p}. \tag{27}$$

When (6) applies, we have $a = 1$ and (26) becomes

$$\tau = \begin{cases} \dfrac{1}{2}\left(\dfrac{1}{p^2} - 1\right) - \ln p, & n = 2, \\ \dfrac{1}{2}\left(\dfrac{1}{p^2} - 1\right) + \dfrac{(n-1)}{(n-2)}\left(1 - p^{n-2}\right), & n \neq 2. \end{cases} \tag{28}$$

These leading-order terms have previously been obtained by Hu (**13**) and King (**39**) in the context of silicon oxidation and Cohen and Erneux (**9**) for solvent penetration in polymers.

2.4.2 *Small Stefan number.* In the limit of small Stefan number ($\lambda \to 0$), there are two relevant timescales, the first being $t = O(\lambda^2)$ and with the second depending on the behaviour of $F(u)$ for small $u$.

Introducing the scalings

$$t = \lambda^2\hat{t}, \qquad x = \lambda\hat{x}, \qquad s = \lambda\hat{s},$$

and posing

$$u \sim \hat{u}_0(\hat{x},\hat{t}), \qquad \hat{s} \sim \hat{s}_0(\hat{t}) \qquad \text{as } \lambda \to 0,$$

on the first of these timescales we obtain at leading order the zero Stefan number problem:

$$\text{in } 0 < \hat{x} < \hat{s}_0(\hat{t}) \qquad \frac{\partial \hat{u}_0}{\partial \hat{t}} = \frac{\partial^2 \hat{u}_0}{\partial \hat{x}^2}, \tag{29}$$

$$\text{on } \hat{x} = 0 \qquad \hat{u}_0 = 1, \tag{30}$$

$$\text{on } \hat{x} = \hat{s}_0(\hat{t}) \qquad \hat{s}_0' = F\left(\hat{u}_0\right), \qquad \frac{\partial \hat{u}_0}{\partial \hat{x}} = -\hat{u}_0\hat{s}_0', \tag{31}$$

$$\text{at } \hat{t} = 0 \qquad \hat{s}_0 = 0, \tag{32}$$

Downloaded from https://academic.oup.com/qjmam/article/56/1/139/1836811 by guest on 21 August 2022

where the prime denotes $d/d\hat{t}$. In the reformulation corresponding to (11) to (14), the moving-boundary conditions read

$$\text{on } \hat{x} = \hat{s}_0(\hat{t}) \qquad \hat{v}_0 = 0, \qquad \hat{s}_0' = F\left(\frac{\partial \hat{v}_0}{\partial \hat{x}}\right), \tag{33}$$

representing a generalization of the classical Stefan problem involving a nonlinear Stefan condition. While the system (29) to (32) cannot be solved analytically, asymptotic behaviours for small and large time may be obtained. As $\hat{t} \to 0$ we have

$$\hat{s}_0(\hat{t}) = a\,\hat{t} - \tfrac{1}{2}\,a^2\,b\,\hat{t}^2 + O(\hat{t}^3), \tag{34}$$

$$u_0(x, \hat{t}) = 1 - a\,\hat{x} + O(\hat{t}^2) \qquad \text{for } \hat{x} = O(\hat{t}),\ 0 < \hat{x}/\hat{t} < a, \tag{35}$$

while as $\hat{t} \to +\infty$ we have a singular perturbation problem with two regions, whereby

$$\hat{u}_0 \sim \operatorname{erfc}\left(\hat{x}/2\hat{t}^{\frac{1}{2}}\right) \qquad \text{for } \hat{x} = O(\hat{t}^{\frac{1}{2}}), \tag{36}$$

and

$$\hat{u}_0 \sim G(\hat{s}_0')\exp\left(-\hat{s}_0'\hat{z}\right) \qquad \text{for } \hat{z} = O(1/\hat{s}_0'), \tag{37}$$

where $\hat{z} = \hat{x} - \hat{s}_0(\hat{t})$. Matching these two expressions implies for (22) that

$$\hat{s}_0(\hat{t}) \sim 2\sqrt{\hat{t}}\,\sigma\left(\ln \hat{t}\right) \qquad \text{as } \hat{t} \to \infty, \tag{38}$$

where $\sigma\left(\hat{\tau}\right)$ satisfies

$$\sigma e^{-\hat{\tau}/2} \sim \left(\sqrt{\pi}\sigma e^{\sigma^2}\right)^{-1/n} \qquad \text{as } \hat{\tau} \to \infty, \tag{39}$$

so that

$$\sigma = \left(\frac{n\hat{\tau}}{2}\right)^{\frac{1}{2}}\left(1 - \frac{(n+1)\ln\hat{\tau}}{2n\hat{\tau}} - \frac{(n+1)\ln(\frac{1}{2}n) + \ln\pi}{2n\hat{\tau}}\right) \qquad \text{as } \hat{\tau} \to \infty. \tag{40}$$

The second timescale depends upon the value of $n$ in (22). The case $n = 1$ in (6) has already been considered in (**1**); for arbitrary $n > 0$ this generalizes as follows.

The appropriate second timescale is $\bar{t} = O(1)$, where

$$t = \lambda^{2(1-1/n)}\,\ln(1/\lambda)\,\bar{t}, \qquad s = \lambda^{1-1/n}\,\ln(1/\lambda)\,\bar{s}.$$

There are two regions which need recording. The boundary layer is

$$x = \lambda^{1-1/n}\,\ln^{\frac{1}{2}}(1/\lambda)\,\bar{x},$$

with

$$u \sim \operatorname{erfc}\left(\bar{x}/2\bar{t}^{\frac{1}{2}}\right). \tag{41}$$

The interior layer about the moving boundary has

$$x = \ln^{\frac{1}{2}}(1/\lambda)\,\bar{s}(\bar{t};\lambda) + \frac{\bar{z}}{\ln^{\frac{1}{2}}(1/\lambda)}, \qquad u \sim \lambda\,\bar{u}_0(\bar{z}, \bar{t}),$$

Downloaded from https://academic.oup.com/qjmam/article/56/1/139/1836811 by guest on 21 August 2022

the moving boundary conditions yielding

$$\bar{u}_0 = \left(1 + \left(\bar{s}_0'\right)^n\right) e^{-(\bar{s}_0')z} - 1$$

with the prime now denoting $d/d\bar{t}$. Matching with (41) then requires

$$\bar{s} \sim 2\bar{t}^{\frac{1}{2}} \left(1 - \frac{\ln\ln(1/\lambda)}{4\ln(1/\lambda)} - \frac{\ln\left(\sqrt{\pi}\left(1 + \bar{t}^{-n/2}\right)\right)}{2\ln(1/\lambda)}\right) \quad \text{as } \lambda \to 0, \tag{42}$$

consistent with (40) as $\bar{t} \to 0^+$.

### 2.5 *The limits of small and large n*

2.5.1 *Small n*. Here we briefly describe the asymptotic behaviour in the limit $n \to 0$ in (6). There are two timescales to discuss, the scalings on the first, $T = O(1)$, being

$$u = 1 - nU, \qquad t = nT, \qquad x = nX, \qquad s = nS,$$

so that the leading-order problem takes the quasi-steady form

$$\begin{aligned}
&\text{in } 0 < X < S_0(T) && \frac{\partial^2 U_0}{\partial X^2} = 0, \\
&\text{on } X = 0 && U_0 = 0, \\
&\text{on } X = S_0(T) && \lambda \frac{dS_0}{dT} = e^{-U_0}, \qquad \frac{\partial U_0}{\partial X} = (1+\lambda)\frac{dS_0}{dT},
\end{aligned}$$

so that

$$U_0 = P(T)X, \qquad \frac{dS_0}{dT} = \frac{1}{\lambda} e^{-PS_0} = \frac{P}{(1+\lambda)}$$

from which it follows that $P$ and $S_0$ are given by

$$\frac{1}{2P^2}\left(\frac{1}{2} + \ln\left(\frac{1+\lambda}{\lambda}\right) - \ln P\right) = \frac{T}{(1+\lambda)} + \frac{\lambda^2}{4(1+\lambda)^2}, \qquad S_0 = -\frac{1}{P}\ln\left(\frac{\lambda P}{1+\lambda}\right). \tag{43}$$

The expansion (17) is reproduced by (43) in the limit $T \to 0^+$ (given that for (6) we have $a = 1, b = 1/n$), while as $T \to +\infty$ it follows that

$$P \sim \frac{(1+\lambda)^{\frac{1}{2}} \ln^{\frac{1}{2}} T}{2T^{\frac{1}{2}}}, \qquad S_0 \sim \frac{T^{1/2} \ln^{\frac{1}{2}} T}{(1+\lambda)^{\frac{1}{2}}}, \tag{44}$$

which is almost of the Neumann similarity form.

It follows from (44) that the second timescale is exponentially long, with scalings

$$u = u(\eta, \tau), \qquad S = 2n^{-\frac{1}{2}} T^{\frac{1}{2}} \sigma(\tau), \tag{45}$$

where

$$\eta = n^{\frac{1}{2}} X / 2T^{\frac{1}{2}}, \qquad \tau = n \ln T, \tag{46}$$

Downloaded from https://academic.oup.com/qjmam/article/56/1/139/1836811 by guest on 21 August 2022

implying that

$$\begin{aligned}
&\text{in } 0<\eta<\sigma(\tau) && 4n\frac{\partial u}{\partial \tau}-2\eta\frac{\partial u}{\partial \eta}=\frac{\partial^2 u}{\partial \eta^2}\ ,\\
&\text{at } \eta=0 && u=1,\\
&\text{at } \eta=\sigma(\tau) && \lambda e^{-\tau/2n}n^{-\frac{1}{2}}\left(\sigma+2n\frac{d\sigma}{d\tau}\right)=u^{1/n}, \qquad \frac{du}{d\eta}=-2(u+\lambda)\left(\sigma+2n\frac{d\sigma}{d\tau}\right)
\end{aligned}$$

so at leading order for $\tau = O(1)$ we obtain

$$\begin{aligned}
&\text{in } 0<\eta<\sigma_0(\tau) && -2\eta\frac{\partial u_0}{\partial \eta}=\frac{\partial^2 u_0}{\partial \eta^2}\ ,\\
&\text{at } \eta=0 && u_0=1,\\
&\text{at } \eta=\sigma_0(\tau) && u_0=e^{-\tau/2}, \qquad \frac{du_0}{d\eta}=-2(u_0+\lambda)\sigma_0,
\end{aligned}$$

representing a Neumann similarity solution which is slowly evolving in time. Hence

$$u_0 = 1 - A(\tau)\mathrm{erf}(\eta),$$

with $A$ and $\sigma_0$ given by

$$\left.\begin{aligned}
&\sqrt{\pi}\sigma_0 e^{\sigma_0^2}\mathrm{erf}(\sigma_0)=\frac{(1-e^{-\tau/2})}{(\lambda+e^{-\tau/2})},\\
&A=\frac{(1-e^{-\tau/2})}{\mathrm{erf}(\sigma_0)},
\end{aligned}\right\} \tag{47}$$

matching with (44) as $\tau, \sigma_0 \to 0^+$ and implying $\sigma_0 \to \alpha$ as $\tau \to +\infty$, consistent with (19) to (21). It is worth remarking that in this limit (43) and (47) provide a complete analytical description of the evolution.

2.5.2 *Large n*. We again consider the power-law relation (6) and now investigate the limit $n \to \infty$. Here the moving-boundary condition

$$\text{on } x=s \qquad\qquad \lambda\dot{s}=u^{1/n}$$

essentially implies in the limit $n \to \infty$ that one of the two possibilities $u = O(1) > 0, \lambda\dot{s} \sim 1$ or $\lambda\dot{s} < 1, u = o(1)$ occurs. In consequence the leading-order formulation should be split into two stages, as follows. For $t < t_c$ we have the linear problem

$$s_0 = t/\lambda \tag{48}$$

$$\left.\begin{aligned}
&\text{in } 0<x<t/\lambda && \frac{\partial u_0}{\partial t}=\frac{\partial^2 u_0}{\partial x^2}\ ,\\
&\text{on } x=0 && u_0=1,\\
&\text{on } x=t/\lambda && \frac{\partial u_0}{\partial x}=-(u_0+\lambda)/\lambda,
\end{aligned}\right\} \tag{49}$$

Downloaded from https://academic.oup.com/qjmam/article/56/1/139/1836811 by guest on 21 August 2022

$t_c$ being determined from (49) via $u_0(t_c/\lambda, t_c) = 0$, with $u_0(t/\lambda, t) > 0$ for $t < t_c$. For $t > t_c$ one instead has the classical Stefan problem

$$\left.\begin{array}{lll} \text{in } 0 < x < s_0(t) & \dfrac{\partial u_0}{\partial t} = \dfrac{\partial^2 u_0}{\partial x^2}\,, & \\ \text{on } x = 0 & u_0 = 1, & \\ \text{on } x = s_0(t) & u_0 = 0, & \dfrac{\partial u_0}{\partial x} = -\lambda \dot{s}_0, \end{array}\right\} \tag{50}$$

with the initial condition being given at $t = t_c$ by the solution to (49) at that time; for $t > t_c$ it is required that $\dot{s}_0 < 1/\lambda$ (so that $-\partial u_0/\partial x$ is greater than one at $x = s_0$ for $t < t_c$ and less than one for $t > t_c$). This scenario is conveniently illustrated by considering the further limit of large $\lambda$ when we obtain $t_c \sim \lambda$ with

$$\left.\begin{array}{llll} s_0 \sim t/\lambda, & u_0 \sim 1 - x & \text{for } t < \lambda, & \\ s_0 \sim (2t/\lambda - 1)^{\frac{1}{2}}, & u_0 \sim 1 - x/s_0 & \text{for } t > \lambda\,; & \end{array}\right\} \tag{51}$$

for (49) to (50) we have $\dot{s}_0$, as well as $s_0$, continuous at $t = t_c$.

The smooth transition between (49) to (50) proceeds as follows. The behaviour of (49) is analytic at $t = t_c$ because $u_0(t/\lambda, t) = 0$ has no special status in that formulation so, in particular,

$$\text{at } x = t/\lambda \qquad u_0 \sim K(t_c - t), \quad \frac{\partial u_0}{\partial x} \sim -1 - \frac{K}{\lambda}(t_c - t) \qquad \text{as } t \to t_c^- \tag{52}$$

for some positive constant $K$. The transition scalings take the form

$$t = t_c + \frac{\tau}{n}, \qquad x = s(t) + \frac{z}{n}, \qquad s(t) \sim s(t_c) + \frac{1}{n}\dot{s}(t_c)\tau + \frac{1}{n^2}S(\tau),$$

with $s(t_c) \sim t_c/\lambda, \dot{s}(t_c) \sim 1/\lambda$ and $u \sim (-z + U(\tau))/n$ for some $U(\tau)$; including appropriate correction terms using (52) in the matching (but omitting details), we obtain from the moving-boundary conditions that

$$\lambda \frac{dS}{d\tau} = \ln U, \qquad \lambda \frac{dS}{d\tau} + \frac{1}{\lambda}U = -\frac{K}{\lambda}\tau,$$

so that

$$\ln U + \frac{1}{\lambda}U = -\frac{K}{\lambda}\tau.$$

Hence

$$U \sim K(-\tau), \quad \lambda S \sim -((-\tau)\ln(-\tau) + (\ln K - 1)(-\tau)) \qquad \text{as } \tau \to -\infty,$$

together with

$$U \sim e^{-K\tau/\lambda}, \quad S \sim -\frac{K\tau^2}{2\lambda^2} \qquad \text{as } \tau \to +\infty\,;$$

for $t > t_c$, $u$ is exponentially small at $x = s(t)$.

Downloaded from https://academic.oup.com/qjmam/article/56/1/139/1836811 by guest on 21 August 2022

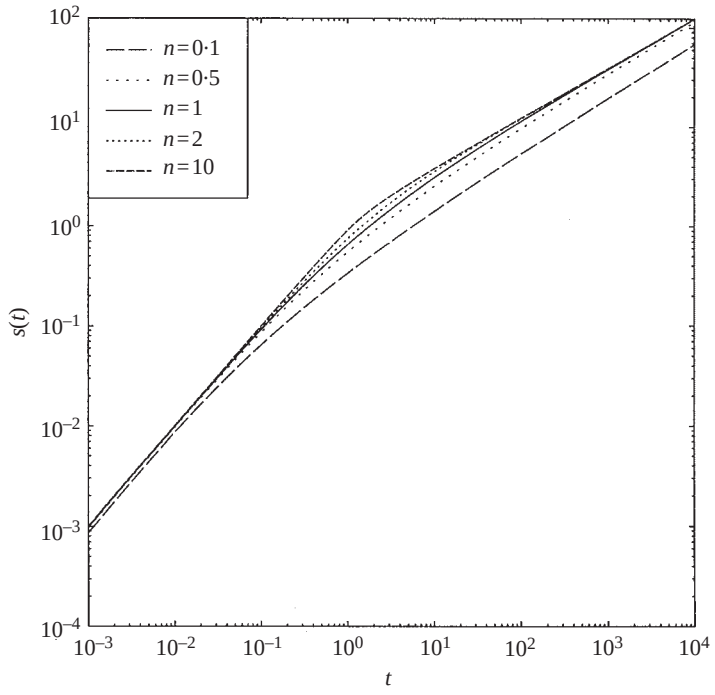


**Fig. 1** Illustration of the evolution of the moving boundary $s(t)$ determined by the numerical solution of (1) to (4) with (6) for the values of $n$ as shown

### 2.6 *Numerical solutions*

Here we illustrate numerically certain features of the system (1) to (4) using the power-law form (6) for the kinetic condition. The explicit front-tracking scheme based on the method of lines considered in Fasano *et al.* (**29**), is used to solve the system numerically.

Figure 1 illustrates the monotonic variation of the position of the moving boundary with the exponent $n$ with the Stefan number fixed at $\lambda = 1$. The small- and large-time asymptotics for each $n$ are qualitatively similar to the linear case $n = 1$ shown in (**1**). The relative insensitivity of the growth of the boundary with $n$ is a feature worth noting and has been a contributory factor in the difficulty in determining the oxide growth law in silicon oxidation.

Figure 2 shows for the small fixed value $n = 0{\cdot}1$ of the algebraic exponent the variation of the boundary growth with the Stefan number $\lambda$. Also shown for each $\lambda$ are the small-$n$ asymptotics on the two dominant timescales, namely (43) and (45) with (47). The asymptotic approximation (43) on the shorter timescale is valid after a short initial transient of $O(n/\lambda)$ which becomes progressively longer as $\lambda$ decreases, as illustrated by the departure of the asymptotic approximation from the full numerical solution at small times.

Figure 3 illustrates the boundary growth for large exponent $n = 10$ with varying values of $\lambda$; the rather abrupt switch at $t = t_c$ described in section 2.5.2 is clearly demonstrated.

Downloaded from https://academic.oup.com/qjmam/article/56/1/139/1836811 by guest on 21 August 2022

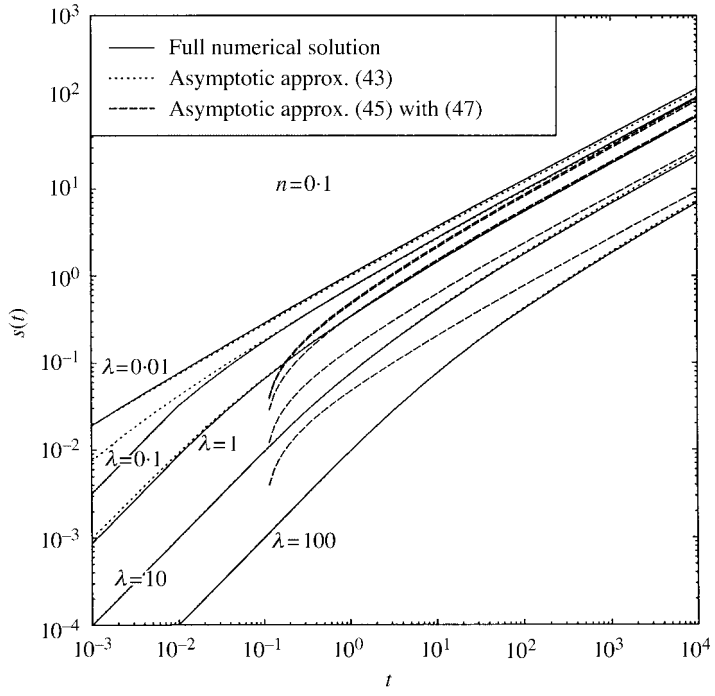


**Fig. 2** Illustration of the evolution of the moving boundary $s(t)$ with the power-law kinetic term (6) in the case $n = 0{\cdot}1$ for the Stefan numbers $\lambda = 0{\cdot}01$, $0{\cdot}1$, 1, 10 and 100. For each $\lambda$ the solid line represents the full numerical solution, whilst next to it, the asymptotic approximations on the two dominant timescales for small $n$ are shown, namely (43) by the dotted lines and (45) with (47) by the dashed lines

## 3. Two-dimensional problems

### 3.1 *Formulation of the mask edge problem*

To illustrate multi-dimensional behaviour, we consider a two-dimensional mask edge problem in which the moving boundary encroaches over a mask. Such scenarios are of particular practical relevance in the silicon oxidation context; see, for example, (**10**, **40**). The initial-boundary-value problem we study is

$$\left.\begin{array}{ll} \text{in } 0 < y < f(x,t), -\infty < x < +\infty & \dfrac{\partial u}{\partial t} = \dfrac{\partial^2 u}{\partial x^2} + \dfrac{\partial^2 u}{\partial y^2}\ , \\ \text{on } y = 0,\ x < 0 & u = 1\ , \\ \text{on } y = 0,\ x > 0 & \dfrac{\partial u}{\partial y} = 0\ , \\ \text{on } y = f(x,t) & \dfrac{\partial u}{\partial n} + v_n(\lambda + u) = 0, \quad u = G(\lambda v_n)\ , \end{array}\right\} \tag{53}$$

Downloaded from https://academic.oup.com/qjmam/article/56/1/139/1836811 by guest on 21 August 2022

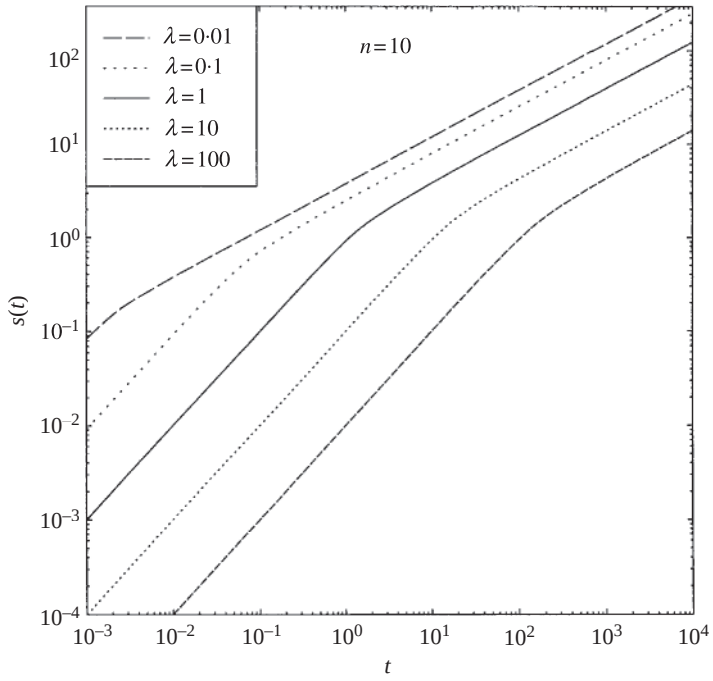


**Fig. 3** Illustration of the evolution of the moving boundary $s(t)$ with the algebraic kinetic term (6) in the case $n = 10$ for various values of the Stefan number $\lambda$

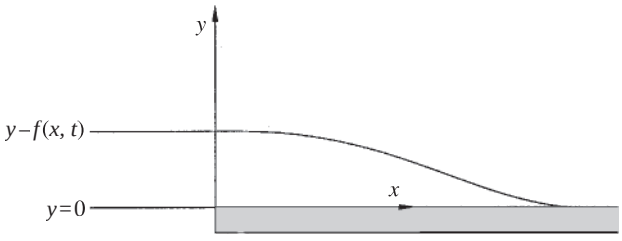


**Fig. 4** A configuration sketch for the two-dimensional mask edge problem

where $v_n$ is the outward normal velocity of the moving boundary and $\partial/\partial n$ denotes the derivative in the outward normal direction, so that

$$v_n = \frac{\partial f}{\partial t} \Big/ \left(1 + \left(\frac{\partial f}{\partial x}\right)^2\right)^{\frac{1}{2}}, \qquad \frac{\partial u}{\partial n} = \left(\frac{\partial u}{\partial y} - \frac{\partial f}{\partial x}\frac{\partial u}{\partial x}\right) \Big/ \left(1 + \left(\frac{\partial f}{\partial x}\right)^2\right)^{\frac{1}{2}}.$$

Downloaded from https://academic.oup.com/qjmam/article/56/1/139/1836811 by guest on 21 August 2022

The surface $y = 0$ is covered by an insulating mask for $x > 0$, while the surface temperature is held fixed for $x < 0$. The configuration is illustrated in Fig. 4. As in (**1**), of the infinite number of solutions that are possible when $f(x, 0) = 0$ for sufficiently large $x$, there are two that are of most interest. We start in section 3.2 by discussing the small-time behaviour of the solution which arises on taking the limit $\epsilon \to 0$ of the case in which there is a uniform initial layer $f(x, 0) = \epsilon^2$, with $0 < \epsilon \ll 1$, and $u(x, y, 0) = 0$. This layer provides a 'crack' along which diffusion can take place and the moving boundary initially propagates extremely rapidly over the mask $y = 0, x > 0$. We then discuss in section 3.3 the small-time behaviour of a second type of solution for which there is no such crack. As in (**1**), these two solutions represent the extremes of an infinite family of possible solutions; such non-uniqueness issues arise much more generally when the moving boundary meets a fixed one, it being necessary to prescribe a suitable (for example, contact-angle) condition at such a point for the problem to be correctly specified.

### 3.2 *'Reaction-controlled' behaviour*

We write

$$x = \epsilon^2 \hat{x}, \qquad y = \epsilon^2 \hat{y}, \qquad f = \epsilon^2 \hat{f}, \qquad t = \epsilon^2 \hat{t},$$

and for $\hat{x} = O(1)$, $\hat{t} = O(1)$ we have

$$u \sim 1, \qquad \hat{f} \sim \hat{f}_0(\hat{x}, \hat{t})$$

with

$$\frac{\partial \hat{f}_0}{\partial \hat{t}} = \frac{a}{\lambda} \left( 1 + \left( \frac{\partial \hat{f}_0}{\partial \hat{x}} \right)^2 \right)^{\frac{1}{2}}, \tag{54}$$

$$\hat{f}_0 = 1 \qquad \text{at } \hat{t} = 0,$$

so that

$$\hat{f}_0 = 1 + \frac{a\,\hat{t}}{\lambda}. \tag{55}$$

The more important region is beneath the mask, with $\hat{X} \equiv \epsilon \hat{x} = O(1)$, $\hat{X} > 0$, in which

$$u \sim u_0(\hat{X}, \hat{t}), \qquad \frac{\partial u}{\partial \hat{y}} \sim \epsilon^2 \left( \frac{\partial u_0}{\partial \hat{t}} - \frac{\partial^2 u_0}{\partial \hat{X}^2} \right) \hat{y}$$

and, writing $\hat{f} \sim f_0(\hat{X}, \hat{t})$, the moving-boundary conditions yield (cf. (**1**))

$$\lambda \frac{\partial f_0}{\partial \hat{t}} = \frac{\partial}{\partial \hat{X}} \left( f_0 \frac{\partial u_0}{\partial \hat{X}} \right) - \frac{\partial}{\partial \hat{t}} \left( f_0 u_0 \right), \qquad G\left( \lambda \frac{\partial f_0}{\partial \hat{t}} \right) = u_0, \tag{56}$$

so that matching with (55) gives the nonlinear evolution equation

$$\frac{\partial}{\partial \hat{t}} \left( f_0 \left( \lambda + G\left( \lambda \frac{\partial f_0}{\partial \hat{t}} \right) \right) \right) = \frac{\partial}{\partial \hat{X}} \left( f_0 \frac{\partial}{\partial \hat{X}} \left( G\left( \lambda \frac{\partial f_0}{\partial \hat{t}} \right) \right) \right), \tag{57}$$

Downloaded from https://academic.oup.com/qjmam/article/56/1/139/1836811 by guest on 21 August 2022

subject to

$$\left.\begin{array}{ll} \text{at } \hat{t}=0 & f_0=1,\ \dfrac{\partial f_0}{\partial \hat{t}}=0, \\ \text{on } \hat{X}=0 & f_0=1+\dfrac{a\,\hat{t}}{\lambda}, \\ \text{as } \hat{X}\to+\infty & f_0\to 1. \end{array}\right\} \tag{58}$$

The leading-order behaviour of (57), (58) for any suitable $t$ is given as $\hat{t}\to+\infty$, for $\hat{X}=O(\hat{t}^{\frac{1}{2}})$, by the (compactly supported) similarity solution

$$f_0=\hat{t}\,g(\hat{X}/\hat{t}^{\frac{1}{2}})$$

with, when $F$ takes the power-law form (6), $g(\eta)$ being given by the free-boundary problem

$$\left.\begin{array}{ll} & g\left(1+\lambda^{n-1}\left(g-\dfrac{\eta}{2}\dfrac{dg}{d\eta}\right)^n\right)-\dfrac{\eta}{2}\dfrac{d}{d\eta}\left(g\left(1+\lambda^{n-1}\left(g-\dfrac{\eta}{2}\dfrac{dg}{d\eta}\right)^n\right)\right) \\ & \qquad\qquad =\lambda^{n-1}\dfrac{d}{d\eta}\left(g\dfrac{d}{d\eta}\left(g-\dfrac{\eta}{2}\dfrac{dg}{d\eta}\right)^n\right), \\ \text{on } \eta=0 & g=1/\lambda, \\ \text{at } \eta=\eta_0 & g=\dfrac{dg}{d\eta}=0. \end{array}\right\} \tag{59}$$

For $\epsilon=0$, $f(x,t)\sim t\,g(x/t^{\frac{1}{2}})$ as $t\to 0^+$, with $g(\eta)$ given by (59), provides the small-time behaviour of one of the extreme solutions to (53), namely the one with zero contact angle. The local behaviour as $\eta\to\eta_0^-$ takes the form

$$g\sim\frac{n}{n+1}\left(\frac{\lambda\eta_0}{2}\right)^{(1-n)/n}(\eta_0-\eta)^{(n+1)/n}; \tag{60}$$

this can be exploited in solving (59) numerically, as follows. We write

$$\eta=\eta_0(1-\xi),\qquad g=\eta_0^{\frac{2}{n}}\,\lambda^{(1-n)/n}\,h,$$

and specify $\eta_0$ to give an initial-value problem for $h(\xi)$, with $h(1)=1/\left(\lambda\eta_0^2\right)^{1/n}$ then being used to determine $\lambda$ for that value of $\eta_0$. Figure 5 illustrates the function $g$ for a selected range of values of $n$ at four values representative of small, intermediate and large $\lambda$. At each value of $\lambda$ the contrasting behaviour in the change in convexity of the function with the exponent $n$ is demonstrated. Figure 6 illustrates the relative insensitivity in the variation of the position of the free boundary $\eta_0$ at each value of $\lambda$ to the value of the exponent $n$.

As $\lambda\to\infty$, the scalings

$$g=\frac{\hat{g}}{\lambda},\qquad \eta=\frac{\hat{\eta}}{\lambda^{\frac{1}{2}}},\qquad \eta_0=\frac{\hat{\eta}_0}{\lambda^{\frac{1}{2}}} \tag{61}$$

Downloaded from https://academic.oup.com/qjmam/article/56/1/139/1836811 by guest on 21 August 2022

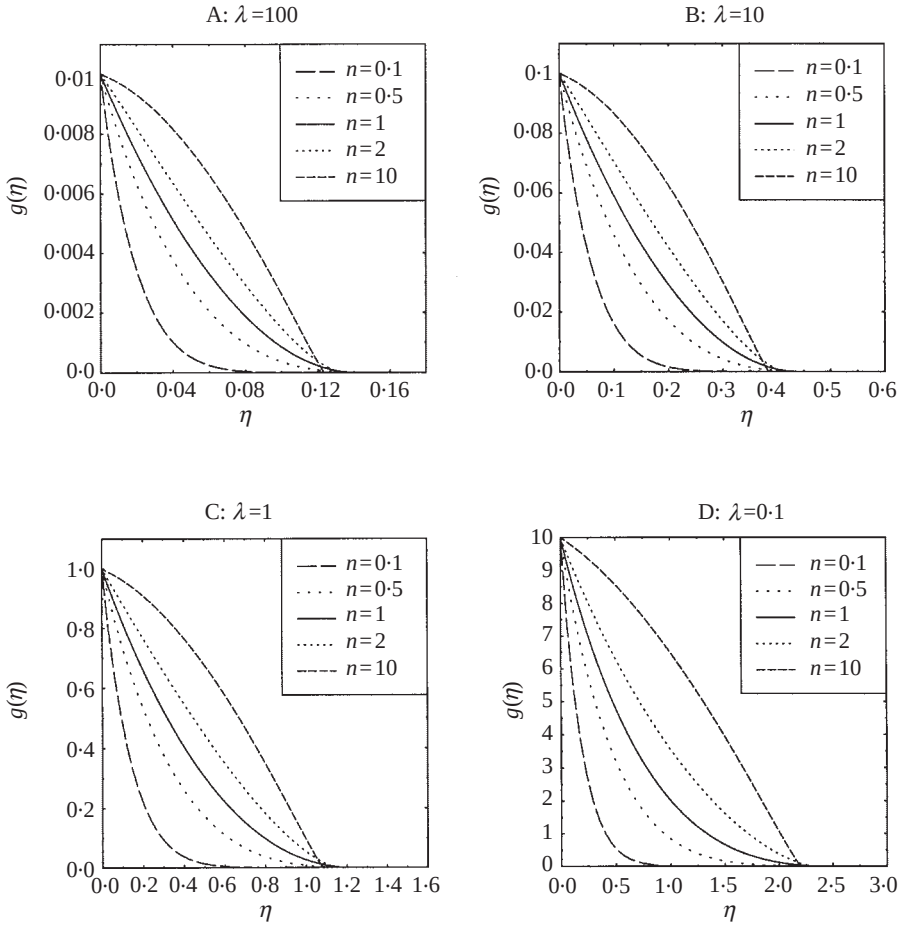


**Fig. 5** The solution $g(\eta)$ to (59) for selected values of $n$ in the power-law kinetic term (6) for each of the cases $\lambda = 100, 10, 1$ and $0{\cdot}1$

give to leading order

$$\left.\begin{array}{ll} & \hat{g}_0 - \dfrac{\hat{\eta}}{2}\dfrac{d\hat{g}_0}{d\hat{\eta}} = \dfrac{d}{d\hat{\eta}}\left(\hat{g}_0\dfrac{d}{d\hat{\eta}}\left(\left(\hat{g}_0 - \dfrac{\hat{\eta}}{2}\dfrac{d\hat{g}_0}{d\hat{\eta}}\right)^n\right)\right), \\ \text{at } \hat{\eta} = 0 & \hat{g}_0 = 1, \\ \text{as } \hat{\eta} \to \hat{\eta}_0^- & \hat{g}_0 \sim \dfrac{n}{n+1}\left(\dfrac{\hat{\eta}_0}{2}\right)^{(1-n)/n}\left(\hat{\eta}_0 - \hat{\eta}\right)^{(n+1)/n}, \end{array}\right\} \tag{62}$$

but an explicit solution seems to be available only for $n = 1$; the scalings are useful, however, in indicating how $\eta_0$ decays with $\lambda$.

Downloaded from https://academic.oup.com/qjmam/article/56/1/139/1836811 by guest on 21 August 2022

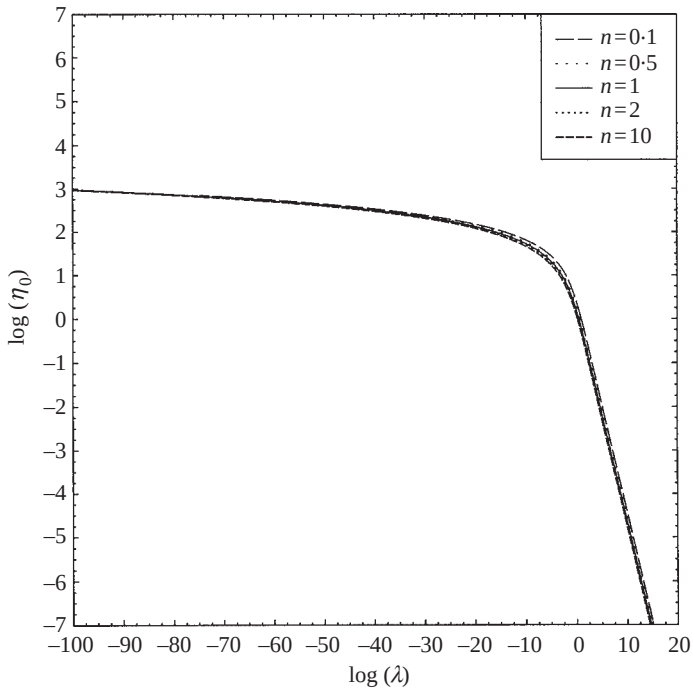


**Fig. 6** A numerical plot of the position of the free boundary $\eta_0$ in (59) with the Stefan number $\lambda$ for selected values of $n$ with the power-law kinetic term (6)

For $\lambda \to 0$ the rescaling $g = \hat{g}/\lambda$ holds in the outer region $\eta = O(1)$, in which $\hat{g} \sim \hat{g}_0(\eta)$ with the 'zero Stefan number' solution $\hat{g}_0$ satisfying

$$\left.\begin{aligned} &\hat{g}_0\left(\hat{g}_0 - \frac{\eta}{2}\frac{d\hat{g}_0}{d\eta}\right)^n - \frac{\eta}{2}\frac{d}{d\eta}\left(\hat{g}_0\left(\hat{g}_0 - \frac{\eta}{2}\frac{d\hat{g}_0}{d\eta}\right)^n\right) = \frac{d}{d\eta}\left(\hat{g}_0\frac{d}{d\eta}\left(\hat{g}_0 - \frac{\eta}{2}\frac{d\hat{g}_0}{d\eta}\right)^n\right), \\ &\text{on } \eta = 0 \qquad \hat{g}_0 = 1, \\ &\text{as } \eta \to +\infty \quad \hat{g}_0 \to 0, \end{aligned}\right\} \tag{63}$$

with $\hat{g}_0 > 0$ holding for all finite $\eta$. The far-field behaviour of (63) can be shown to be

$$\hat{g}_0 \sim A_0\,\eta^{\alpha}\,e^{-\beta\eta^2} \qquad \text{as } \eta \to +\infty, \tag{64}$$

where

$$\alpha = -\frac{2n+5}{n+1}, \qquad \beta = \frac{1}{4n}, \tag{65}$$

and $A_0(n)$ is a constant which must be determined as part of the solution to (63). The scalings in an interior layer at the moving boundary are then

$$\eta = \ln^{\frac{1}{2}}(1/\lambda)\,S(\lambda) + \frac{z}{\ln^{\frac{1}{2}}(1/\lambda)}, \qquad g \sim \frac{G_0}{\lambda^{(n-1)/n}\ln(1/\lambda)}, \tag{66}$$

Downloaded from https://academic.oup.com/qjmam/article/56/1/139/1836811 by guest on 21 August 2022

where

$$S(\lambda) = 2\left(1 + \frac{n(\alpha+2)\,\ln\ln(1/\lambda)}{4\ln(1/\lambda)} + \frac{n\,(\ln(A_0/n) + \alpha\ln 2)}{2\ln(1/\lambda)}\right) \tag{67}$$

gives from (64) the matching condition

$$G_0 \sim n\,e^{-z/n} \qquad \text{as } z \to -\infty. \tag{68}$$

From (66) it follows that $G_0(z)$ satisfies the autonomous equation

$$-\frac{d}{dz}\left(G_0\left(1+\left(-\frac{dG_0}{dz}\right)^n\right)\right) = \frac{d}{dz}\left(G_0\frac{d}{dz}\left(-\frac{dG_0}{dz}\right)^n\right),$$

which represents a travelling wave balance in (57), so that (68) and the moving-boundary conditions yield

$$G_0 = \int_0^{-z} \left(e^{\xi}-1\right)^{1/n}\,d\xi \quad \text{for } z<0, \qquad \eta_0 \sim S(\lambda)\ln^{\frac{1}{2}}(1/\lambda). \tag{69}$$

The small- and large-$\lambda$ asymptotics can qualitatively be seen in the numerical results of Fig. 6 where the weak dependence of $\eta_0$ on $n$ is evident; quantitative comparison leads to curves that are almost indistinguishable (the $n = 1$ case is shown in (**1**, Fig. 6)). Moreover, the small-$\lambda$ behaviour is numerically seen to be more sensitive to $n$ than the large-$\lambda$ behaviour, in agreement with (69), (67) and (61), (62).

### 3.3 *Small-time behaviour—no initial 'crack'*

Here we note the other extreme case in which the moving boundary meets the mask at an angle of $\frac{1}{2}\pi$, in which case $y = 0$, $x > 0$ may correspond to a line of symmetry rather than a physical boundary. The small-time behaviour is then of the same form as in the linear kinetic undercooling case given in (**1**, section 6.3), being governed by the hyperbolic evolution equation (54) except that the Stefan number $\lambda$ in that analysis is replaced by $\lambda/a$. The solution may be recorded as follows:

$$\hat{f}_0 = \begin{cases} \dfrac{a\hat{t}}{\lambda} & \text{if } \hat{x} < 0, \\[2ex] \dfrac{a\hat{t}}{\lambda}\left(1-\left(\dfrac{\lambda\hat{x}}{a\hat{t}}\right)^2\right)_+^{\frac{1}{2}} & \text{if } \hat{x} > 0. \end{cases}$$

### 3.4 *Other limits*

The $G$ term in (53) is negligible for large $t$, so the behaviour as $t \to +\infty$ is as outlined in (**1**). For $\lambda \to \infty$, the scalings $t = \lambda\,\hat{t}$, $v_n = \hat{v}_n/\lambda$ apply, so that the $\partial u/\partial t$ term is negligible, giving a Hele-Shaw problem with a nonlinear kinetic undercooling boundary condition. This limit is particularly appropriate to the case of silicon oxidation, (62) providing a concise description of the shape of the resulting 'bird's beak' (cf. (**10**)). We return to such matters below. The behaviour as $\lambda \to 0$ is relatively insensitive to the form of $G$ (cf. section 2.4.2) and we do not go into details.

Downloaded from https://academic.oup.com/qjmam/article/56/1/139/1836811 by guest on 21 August 2022

## 4. Discussion

As is clear from (17), (19) and Fig. 1, the growth behaviour in one dimension is rather insensitive to the precise form of $F(u)$ and this has hindered the experimental determination of $F(u)$. By contrast, it is evident from Fig. 5 that profiles of two-dimensional growth under a mask edge depends strongly on the form of $F(u)$. It is therefore worth describing a technique (analogous to the Boltzmann–Matano method for determining nonlinear diffusivities; see Tuck (**41**), for example) for enabling the kinetic undercooling relation to be deduced from the experimental determination of two-dimensional interfaces in the reaction-controlled regime (for example, by high pressure oxidation; see Powell *et al.* (**42**), for instance). For brevity, and because of its relevance to silicon oxidation, we consider only the limit case $\lambda \to \infty$, in which the leading-order problem is quasi-steady, so in dimensional form we have

$$\frac{\partial^2 u}{\partial x^2} + \frac{\partial^2 u}{\partial y^2} = 0 \,,$$

$$\text{on } y = 0 \qquad \frac{\partial u}{\partial y} = 0 \,,$$

$$\text{on } y = f \qquad \beta v_n = -D\frac{\partial u}{\partial n} \,, \qquad u = \Phi(v_n),$$

where $\Phi$ is the nonlinear kinetic undercooling relation that we wish to measure (with $\Phi(0) = 0$), $D$ is the oxidant diffusivity and $\beta$ is the number of oxidant molecules reacting with unit volume of silicon (or $\rho L$ in the context of heat conduction, where $\rho$ is density and $L$ is the latent heat). The corresponding dimensional form of (57) is

$$\beta\frac{\partial f}{\partial t} = D\frac{\partial}{\partial x}\left(f\frac{\partial u}{\partial x}\right), \qquad u = \Phi\left(\frac{\partial f}{\partial t}\right)$$

so, writing

$$u = u(x/t^{\frac{1}{2}}), \qquad f = tg(x/t^{\frac{1}{2}}), \qquad v = g - \frac{1}{2}\eta\frac{dg}{d\eta}, \tag{70}$$

we obtain the system

$$\beta v = D\frac{d}{d\eta}\left(g\frac{du}{d\eta}\right), \qquad v = g - \frac{1}{2}\eta\frac{dg}{d\eta}, \qquad u = \Phi(v). \tag{71}$$

Measuring $f(x, t)$ at a given $t$ enables $\eta(v)$ and $g(v)$ to be obtained from (70) and, since for relevant $\Phi(v)$ the solution to (71) is compactly supported, with $g = 0$ for $\eta \geqslant \eta_0$ and

$$\text{as } \eta \to \eta_0^- \qquad g\frac{du}{d\eta} \to 0, \quad v \to 0, \quad g \to 0, \tag{72}$$

it follows from (71) that

$$\phi(v) = \frac{\beta}{Dg(v)}\left(v\eta(v) - \int_0^v \eta(v')dv'\right)\frac{d\eta(v)}{dv}, \tag{73}$$

where $\phi(v) = \Phi'(v)$; the expression (73) thus in principle enables $\Phi(v)$ to be deduced from an experimental profile; it can also be used analytically in an inverse approach whereby $\eta(v)$ is given

Downloaded from https://academic.oup.com/qjmam/article/56/1/139/1836811 by guest on 21 August 2022

(with $\eta(v)$ and $g(v)$ satisfying $\eta(0) = \eta_0$, $g(0) = 0$ with $(1/2(g - v))(dg/dv) = (1/\eta)(d\eta/dv)$ and the corresponding $\Phi(v)$ deduced; the simplest example of this is

$$\eta = \eta_0 - Kv$$

for constant $K$, in which case

$$g = Kv^2/\eta_0, \qquad \phi = K\beta\eta_0/2D, \qquad \Phi = K\beta\eta_0 v/2D,$$

reproducing the linear kinetic undercooling law studied in [1].

The applicability or otherwise of this technique, based on (73), can be assessed if the interface $f(x, t)$ can be measured as a function of time and its level of consistency with the self-similar form in (70) quantified (which requires the experimental conditions to lie in the reaction-controlled regime with the maximum oxide thickness being much greater than it was initially). We emphasize (cf. Fig. 5) that our results illustrate the rather pronounced sensitivity of $f$ on the kinetics, so the proposed method is expected to be effective in practice in extracting the required information from suitable experimental data and the procedure should be significantly more robust than the fits to one-dimensional behaviour pursued in (**12**, **13**, **15**), for instance.

A natural extension of the work presented in this paper is to investigate the two-phase problem. This would be of particular relevance in heat transfer applications (both melting and solidification), where the one-phase approximation may be viewed as artificial. (We emphasize, however, that this is not the case in many mass transfer problems, the silicon oxidation and polymer penetration problems in particular being intrinsically one-phase, since the oxidant or solvent is unable to diffuse significantly into the second phase (cf. (**14**)).) However, many of the approaches discussed here are expected to carry over.

**Acknowledgement**

Financial support is gratefully acknowledged by the first author from the Nuffield Foundation and by the second from the Leverhulme Trust.

**References**

**1.** J. D. Evans and J. R. King, Asymptotic results for the Stefan problem with kinetic undercooling, *Q. Jl Mech. Appl. Math.* **53** (2000) 449–473.
**2.** R. J. Kirkpatrick, G. R. Robinson and J. F. Hays, Kinetics of crystal growth from silicate melts: Anorthite and diopside, *J. Geophys. Res.* **81** (1976) 5715–5720.
**3.** M. G. Worster and R. C. Kerr, The transient-behaviour of alloys solidified from below prior to the formation of chimneys, *J. Fluid Mech.* **269** (1994) 23–44.
**4.** A. B. Crowley, Some remarks on non-equilibrium solidification problems, *Free and Moving Boundary Problems* (ed. K. H. Hoffman and J. Sprekels; Pitman, London 1989).
**5.** G. Astarita and S. Joshi, Sample-dimension effects in the sorption of solvents in polymers—A mathematical model, *J. Membrane Sci.* **4** (1978) 165–182.
**6.** —— and G. C. Sarti, A class of mathematical models for sorption of swelling solvents in glassy polymers, *Polymer Eng. Sci.* **18** (1978) 388–395.
**7.** ——, A class of free boundary problems arising in the analysis of transport phenomena in polymers, *Free Boundary Problems: Theory and Applications*, II (ed. A. Fasano and M. Primicerio; Pitman, London 1983) 602–612.

Downloaded from https://academic.oup.com/qjmam/article/56/1/139/1836811 by guest on 21 August 2022

**8.** A. Fasano and R. Ricci, Penetration of solvents into glassy polymers, *Free Boundary Problems: Applications and Theory*, III, Research Notes in Mathematics 120 (ed. A. Bossavit, A. Damlamian and M. Fremond; Pitman, London 1985) 132–139.
**9.** D. S. Cohen and T. Erneux, Free boundary problems in controlled release pharmaceuticals. I: Diffusion in glassy polymers, *SIAM J. Appl. Math.* **48** (1988) 1451–1465.
**10.** J. R. King, The isolation oxidation of silicon, *ibid.* **49** (1989) 264–280.
**11.** A. B. Tayler and J. R. King, Free boundaries in semi-conductor fabrication, *Free Boundary Problems: Theory and Applications*, II, Pitman Research Notes in Mathematics (ed. K. H. Hoffman and J. Sprekels; Longman Scientific & Technical, London 1990) 243–256.
**12.** J. Blanc, A revised model for the oxidation of silicon by oxygen, *Appl. Phys. Lett.* **33** (1978) 424–426.
**13.** S. M. Hu, New oxide growth law and the thermal oxidation of silicon, *ibid.* **42** (1983) 872–874.
**14.** J. D. Evans and J. R. King, On the derivation of heterogeneous reaction kinetics from a homogeneous reaction model, *SIAM J. Appl. Math.* **60** (2000) 1977–1996.
**15.** S. M. Hu, Thermal oxidation of silicon: chemisorption and linear rate constant, *J. Appl. Phys.* **54** (1984) 1069–1075.
**16.** R. J. Schaefer and M. E. Glicksman, Fully time-dependent theory for the growth of spherical crystal nuclei, *J. Crystal Growth* **5** (1969) 44–58.
**17.** A. Umantsev and S. H. Davis, Growth from a hypercooled melt near absolute stability, *Physical Rev.* A. **45** (1992) 7195–7201.
**18.** W. W. Mullins and R. F. Sekerka, Morphological stability of a particle growing by diffusion or heat flow, *J. Appl. Phys.* **34** (1963) 323–329.
**19.** J. S. Langer, Instabilities and pattern formation in crystal growth, *Rev. Mod. Phys.* **52** (1980) 1–28.
**20.** J. Chadam and P. Ortoleva, The stabilizing effect of surface tension on the development of the free boundary in a planar, one-dimensional, Cauchy–Stefan problem, *IMA J. Appl. Math.* **30** (1983) 57–66.
**21.** ——, S. D. Howison and P. Ortoleva, Existence and stability for spherical crystals growing in a supersaturated solution, *ibid.* **39** (1987) 1–15.
**22.** S. Luckhaus, Solutions for the two-phase Stefan problem with the Gibbs–Thomson law for the melting temperature, *Euro. J. Appl. Math.* **1** (1990) 101–111.
**23.** Q. Zhu, A. Peirce and J. Chadam, Initiation of shape instabilities of free boundaries in planar Cauchy-Stefan problems, *ibid.* **4** (1993) 419–436.
**24.** S. H. Doole, A Stefan-like problem with a kinetic condition and surface tension effects, *Math. Comput. Modelling* **23** (1996) 55–67.
**25.** G. Scianna, Global existence and asymptotic behavior for the radially symmetric case of a two-phase Stefan problem with interfacial energy, *J. Math. Anal. Appl.* **211** (1997) 1–29.
**26.** I. Rubinstein and B. Zaltzman, Morphological instability of similarity solution to the Stefan problem with kinetic undercooling and surface tension, *Quart. Appl. Math.* **56** (1998) 341–354.
**27.** F. Abergel, D. Hilhorst and F. Issard-Roch, On a dissolution-growth problem with surface tension in the neighborhood of a stationary solution, *SIAM. J. Math. Anal.* **24** (1993) 299–316.
**28.** J. F. Scheid, A dissolution-growth problem with surface tension: Local existence and uniqueness, *Appl. Math. Lett.* **8** (1995) 91–95.

Downloaded from https://academic.oup.com/qjmam/article/56/1/139/1836811 by guest on 21 August 2022

**29.** A. Fasano, G. H. Meyer and M. Primicerio, On a problem in the polymer industry: Theoretical and numerical investigation of swelling, *SIAM J. Math. Anal.* **17** (1986) 945–960.
**30.** D. Andreucci and R. Ricci, A free boundary problem arising from sorption of solvents in glassy polymers, *Quart. Appl. Math.* **19** (1987) 649–657.
**31.** K. Gröger and N. Strecker, A free boundary value problem modeling thermal oxidation of silicon, *Zeit. Anal. Anwend.* **7** (1988) 57–66.
**32.** W. Xie, The Stefan problem with a kinetic condition at the free boundary, *SIAM J. Math. Anal.* **21** (1990) 362–373.
**33.** X. Chen and F. Reitich, Local existence and uniqueness of solutions of the Stefan problem with surface tension and kinetic undercooling, *J. Math. Anal. Appl.* **164** (1992) 350–362.
**34.** Ch Charach, B. Zaltzman and I. G. Götz, Interfacial kinetics effect in planar solidification problems without initial undercooling, *Math. Models Methods Appl. Sci.* **4** (1994) 331–354.
**35.** I. G. Götz and B. Zaltzman, Two-phase Stefan problem with supercooling, *SIAM J. Math. Anal.* **26** (1995) 694–714.
**36.** A. Visintin, Stefan problem with a kinetic condition at the free boundary, *Ann. Mat. Pura Appl.* **146** (1987) 97–122.
**37.** Z. Guan and X.-J. Wang, Existence and blow-up of solutions to two-phase nonequilibrium problems, *SIAM J. Math. Anal.* **27** (1996) 1038–1048.
**38.** —— and ——, Critical exponent in a Stefan problem with kinetic condition, *Euro. J. Appl. Math.* **8** (1997) 525–532.
**39.** J. R. King, Mathematical aspects of semiconductor process modelling, D.Phil. Thesis, Oxford University (1986).
**40.** ——, The isolation oxidation of silicon: The reaction-controlled case, *SIAM J. Appl. Math.* **49** (1989) 1064–1080.
**41.** B. Tuck, *Atomic Diffusion in III–V Semiconductors* (Institute of Physics Publishing, Bristol 1988).
**42.** R. J. Powell, J. R. Ligenza and M. S. Schneider, Selective oxidation of silicon in low-temperature high-pressure steam, *IEEE Trans. Electron Dev.* ED **21** (1974) 636–640.

## APPENDIX A

*Slender evolution equation with nonlinear diffusion*

Here we briefly note the generalization to (56) which arises when the diffusion problem in (53) is made nonlinear and a rather general regularization is adopted on the moving boundary; we thus consider

$$\left.\begin{aligned} & \epsilon^2 \frac{\partial u}{\partial \hat{t}} = \frac{\partial}{\partial \hat{y}}\left(D(u)\frac{\partial u}{\partial \hat{y}}\right) + \epsilon^2 \frac{\partial}{\partial \hat{X}}\left(D(u)\frac{\partial u}{\partial \hat{X}}\right), \\ \text{on } \hat{y} = 0,\ \hat{X} > 0 \qquad & \frac{\partial u}{\partial \hat{y}} = 0, \\ \text{on } \hat{y} = \hat{f}(\hat{X}, \hat{t}) \qquad & D(u)\left(\frac{\partial u}{\partial \hat{y}} - \epsilon^2 \frac{\partial \hat{f}}{\partial \hat{X}}\frac{\partial y}{\partial \hat{X}}\right) + \epsilon^2(\lambda + u)\frac{\partial \hat{f}}{\partial \hat{t}} = 0, \qquad u = \Phi(\lambda \hat{v}_n, \sigma\hat{\kappa}), \end{aligned}\right\} \tag{A1}$$

where

$$\hat{v}_n = \frac{\partial \hat{f}}{\partial \hat{t}} \Big/ \left(1 + \epsilon^2\left(\frac{\partial \hat{f}}{\partial \hat{X}}\right)^2\right)^{\frac{1}{2}}, \qquad \hat{\kappa} = -\frac{\partial^2 \hat{f}}{\partial \hat{X}^2} \Big/ \left(1 + \epsilon^2\left(\frac{\partial \hat{f}}{\partial \hat{X}}\right)^2\right)^{\frac{3}{2}}$$

Downloaded from https://academic.oup.com/qjmam/article/56/1/139/1836811 by guest on 21 August 2022

correspond to the normal velocity and curvature of the moving boundary, so that (through $\Phi$) (A1) incorporates general regularizing effects due to both kinetic undercooling and surface energy (with parameter $\sigma$). The generalization of $(56)_1$ is then readily derived in the form

$$\frac{\partial}{\partial \hat{t}}\left((\lambda + u_0) f_0\right) = \frac{\partial}{\partial \hat{X}}\left( f_0 D(u_0) \frac{\partial u_0}{\partial \hat{X}} \right), \tag{A2}$$

independent of the regularization, with the higher-dimensional version taking the form

$$\frac{\partial}{\partial t}\left((\lambda + u) f\right) = \nabla \cdot \left( f D(u) \nabla u \right). \tag{A3}$$

Similarly, $(56)_2$ is replaced by

$$u_0 = \Phi\left( \lambda \frac{\partial f_0}{\partial \hat{t}}, -\sigma \frac{\partial^2 f_0}{\partial \hat{X}^2} \right) \tag{A4}$$

and, in higher dimensions, (A3) is supplemented by

$$u = \Phi\left( \lambda \frac{\partial f}{\partial t}, -\sigma \nabla^2 f \right). \tag{A5}$$

We conclude by mentioning that, somewhat remarkably, the novel evolution system (A2), (A4) admits for any $D$ and $\Phi$ similarity solutions of the form

$$u_0 = U(\hat{X}/(\pm\hat{t})^{\frac{1}{2}}), \qquad f_0 = (\pm t) G(\hat{X}/(\pm\hat{t})^{\frac{1}{2}}),$$

which are of interest in applications (cf. (70)). The $t^1$ behaviour of $f$ is characteristic of reaction-controlled behaviour in the $y$-direction, whereas $x$ scales with $t^{\frac{1}{2}}$, characteristic of diffusion control.

Downloaded from https://academic.oup.com/qjmam/article/56/1/139/1836811 by guest on 21 August 2022